

Figure S1. Improvement in retinal organoid production across multiple hPSC lines using an early pulse of BMP4. (A) Bar graph depicting the fold increase in mean retinal organoid production across seven hPSC lines relative to untreated lines. The p -value was calculated using a one sample Student's t -test against an untreated control mean of 1. (B) Plated EBs at d30 of retinal differentiation (immediately prior to dissection and transfer into suspension cultures) showing the difference in organoid-like structure between BMP4-treated and untreated cultures (scale bar = 100 μ m). (C) Live LM phase images of stage 2 d90 organoids showing clumps of RPE (denoted with asterisks) (scale bar = 50 μ m). (D) Live LM phase images of two representative d200 organoids from the same culture differentiation showing the coexistence of stage 2 organoids with no surface projections (left panel) and stage 3 organoids with surface projections (right panel) (scale bar = 50 μ m).

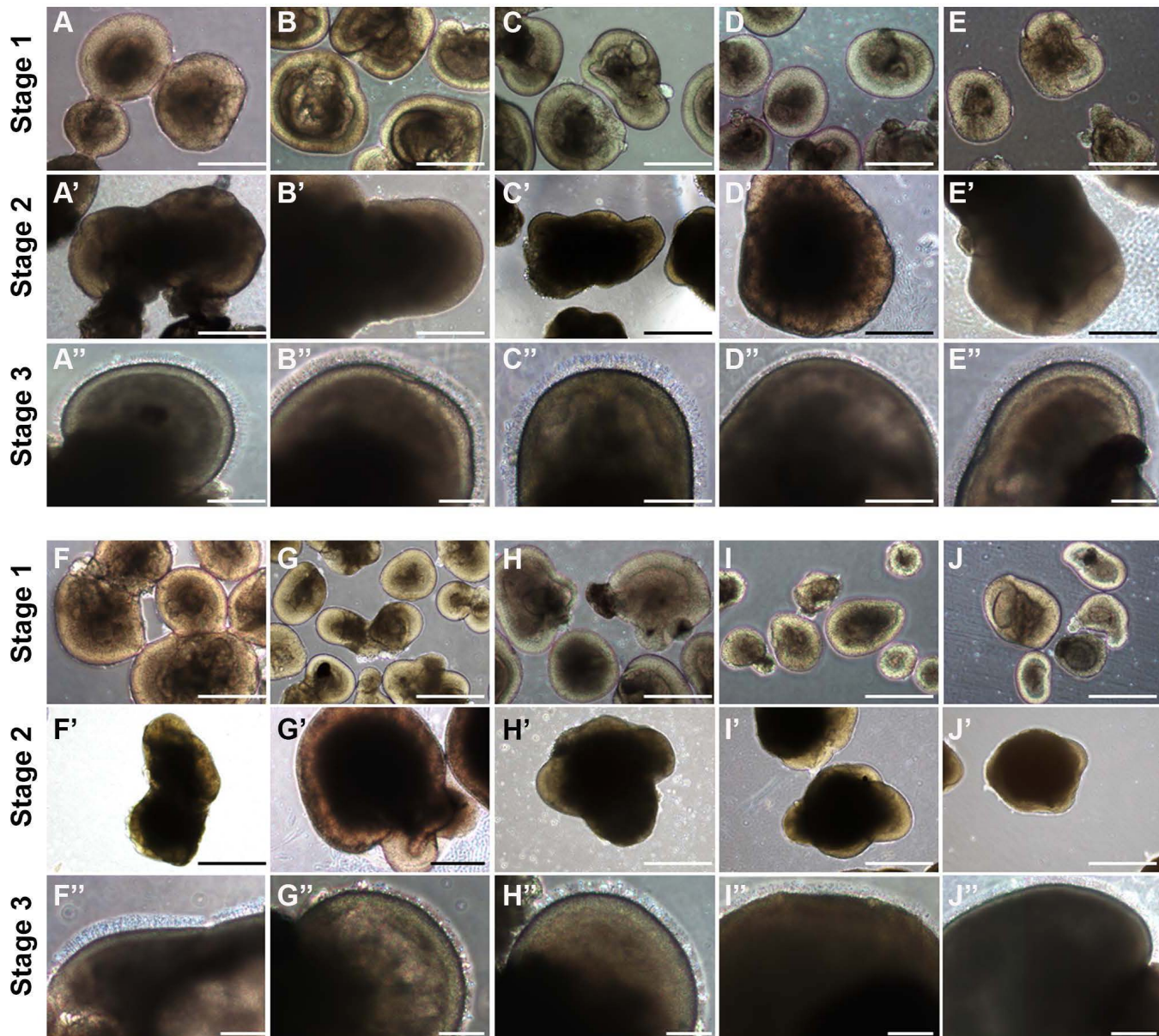


Figure S2. Live LM phase images of the three distinct stages of retinal organoid morphology across 10 hPSC lines. (A-J'') Representative images of stage 1, 2, and 3 organoids are shown for two gene-edited hiPSC lines (A-B''), one gene-edited hESC line (C-C''), four hiPSC lines for patients affected with inherited retinal degenerations (D-G''), and three wildtype hiPSC lines (H-J'') (scale bars = 250 μ m).

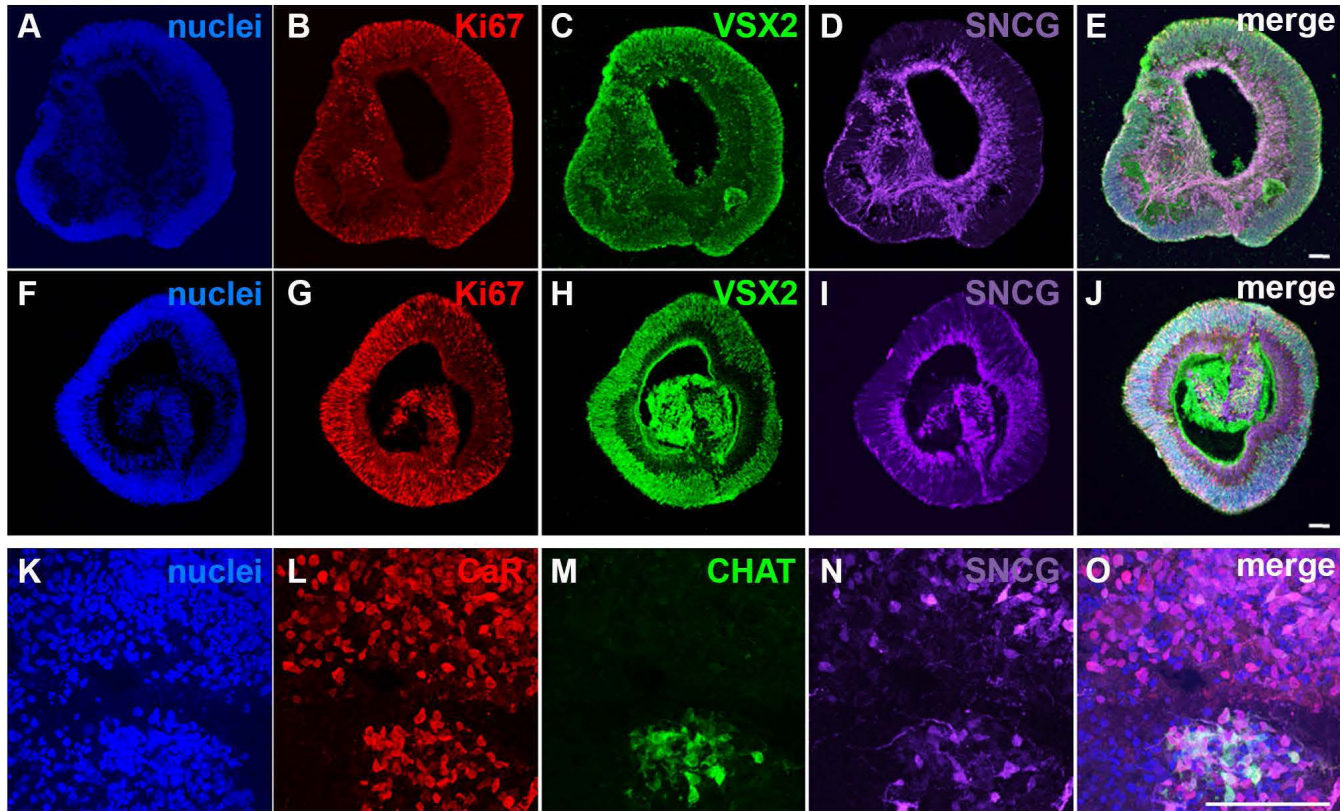


Figure S3. Stage 1 organoid cell composition in additional hPSC lines. (A-J) ICC images of d35 organoids from two additional hPSC lines showing Ki67+/VSX2+ proliferating NRPCs along the outer rim and SNCG+ RGCs on the inside of stage 1 organoids (scale bar = 100 μ m). **(K-O)** ICC images of a d35 stage 1 organoid from an additional hPSC line showing CHAT+ SACs among the SNCG+ RGCs and CaR+ ACs found at this stage (scale bar = 100 μ m).

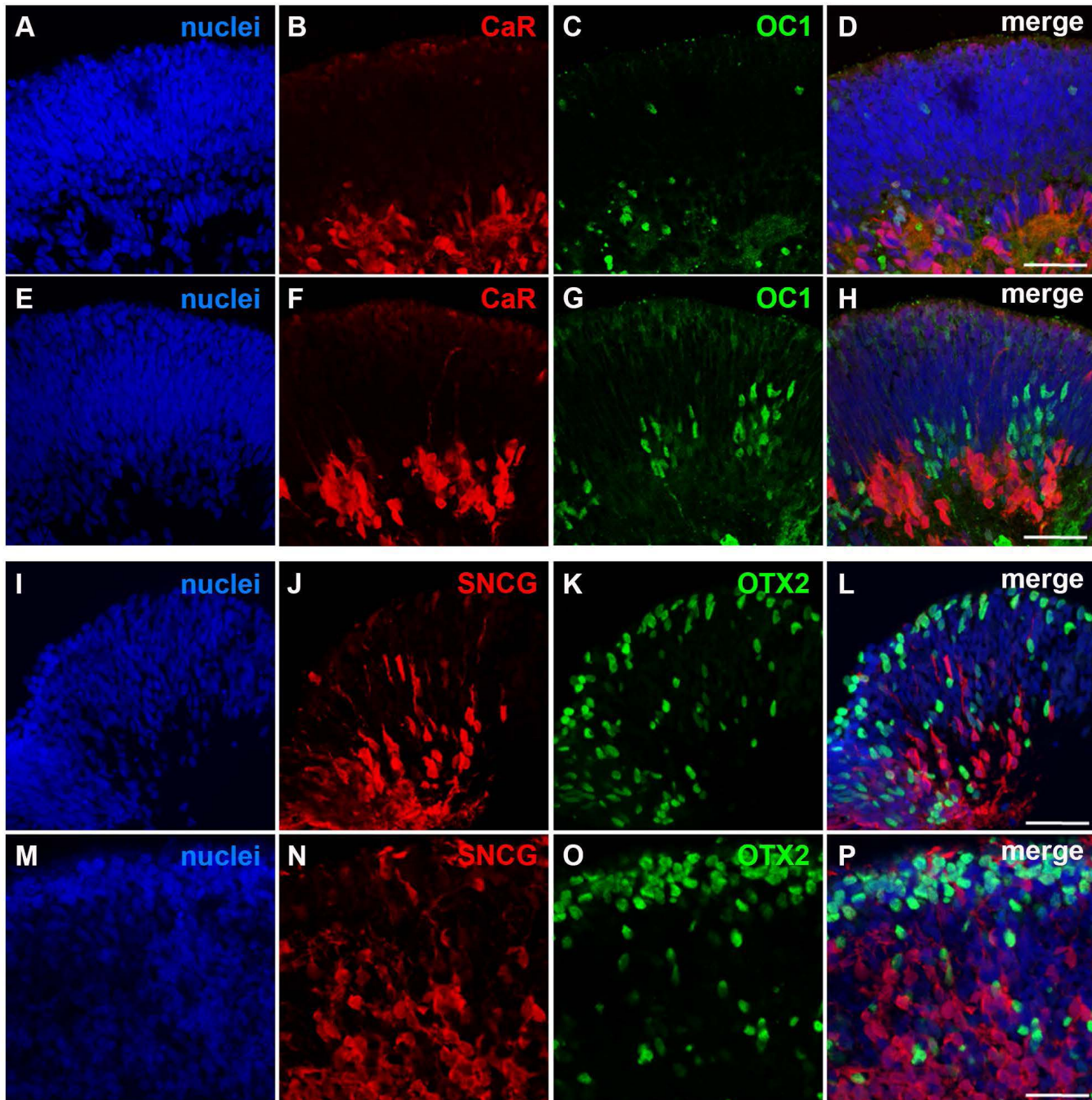


Figure S4. Early stage 2 organoid cell composition in additional hPSC lines. (A-H) ICC images of d80 stage 2 organoids from two additional hPSC lines showing the presence of CaR+ ACs and RGCs and OC1+ HCs. (I-P) ICC images of d74-d80 stage 2 organoids from two additional lines showing the presence of OTX2+ PR progenitors along the outer rim with SNCG+ RGCs located more internally (scale bars = 50 μ m).

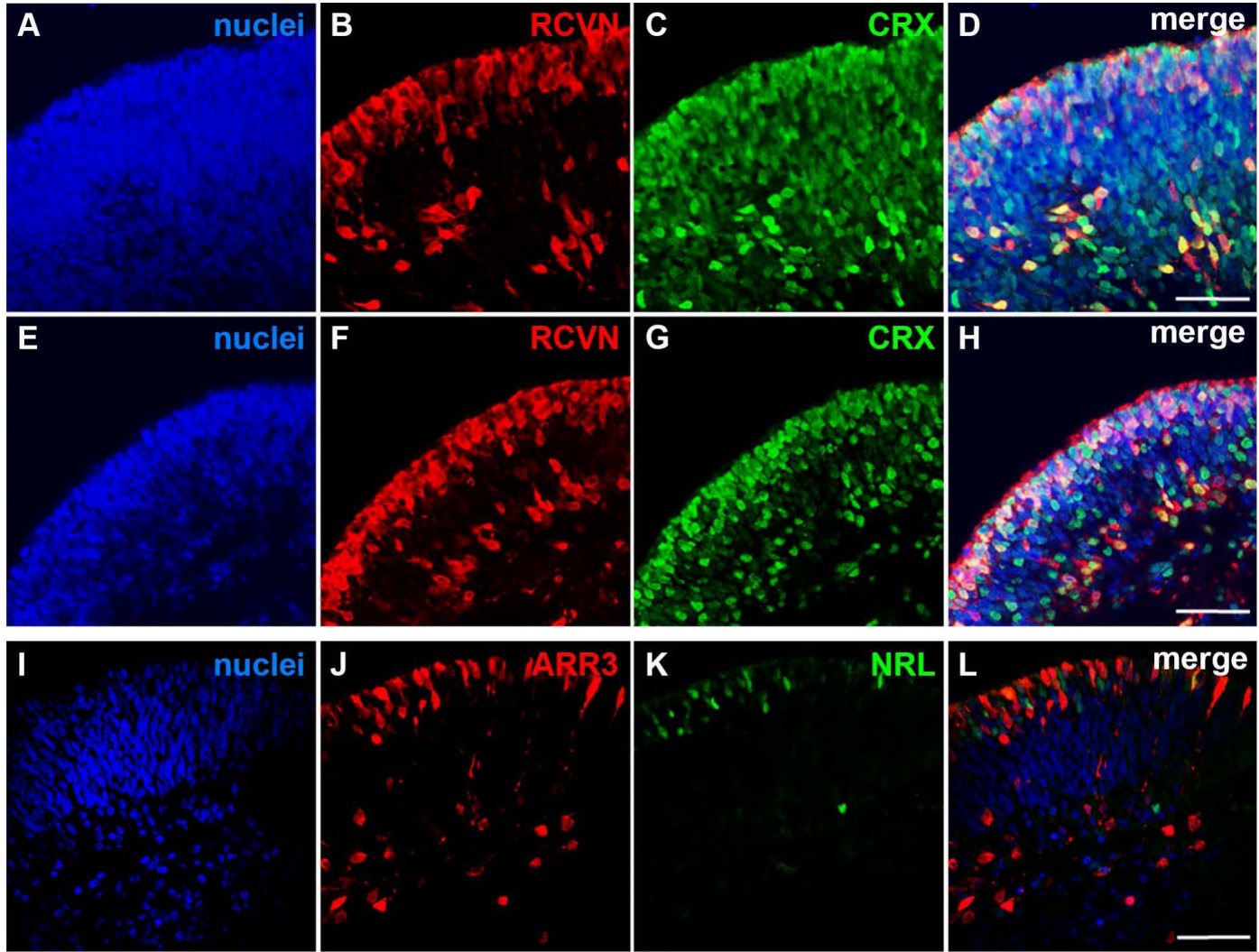


Figure S5. Stage 2 organoid PR composition in additional hPSC lines. (A-H) ICC images of d80 stage 2 organoids from two additional lines showing maturing RCVN+/CRX+ PRs predominantly near the surface. (I-L) ICC image of a d145 stage 2 organoid from an additional line showing the presence of maturing ARR3+ cones and NRL+ rods (scale bars = 50 μ m).

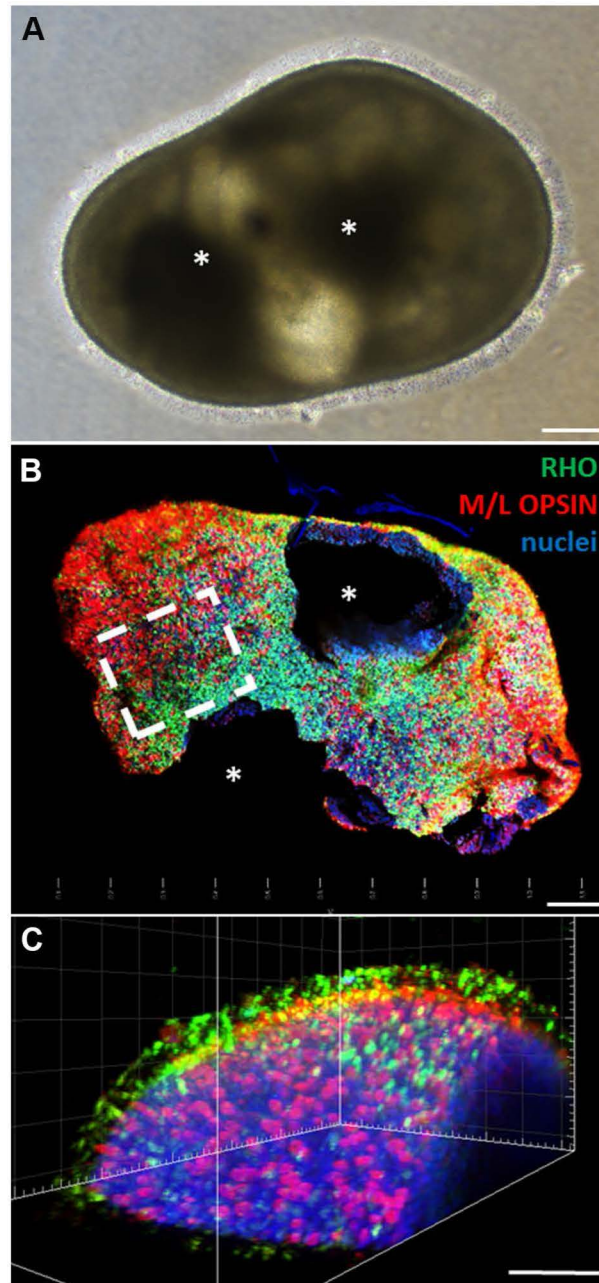


Figure S6. Multiphoton 3D reconstruction of a stage 3 organoid from an additional line showing the surface distribution of rods and cones. (A) Phase LM image of a d345 stage 3 organoid fixed for whole organoid immunostaining and multiphoton imaging. The asterisks mark attached RPE clumps. **(B, C)** Reconstructed multiphoton 3D image of the stage 3 organoid in panel A showing the surface distribution of RHO+ rods and M/L-OPSIN+ cones. The asterisks mark attached RPE clumps and the area within the dashed square is magnified in panel C (scale bars = 100 μ m).

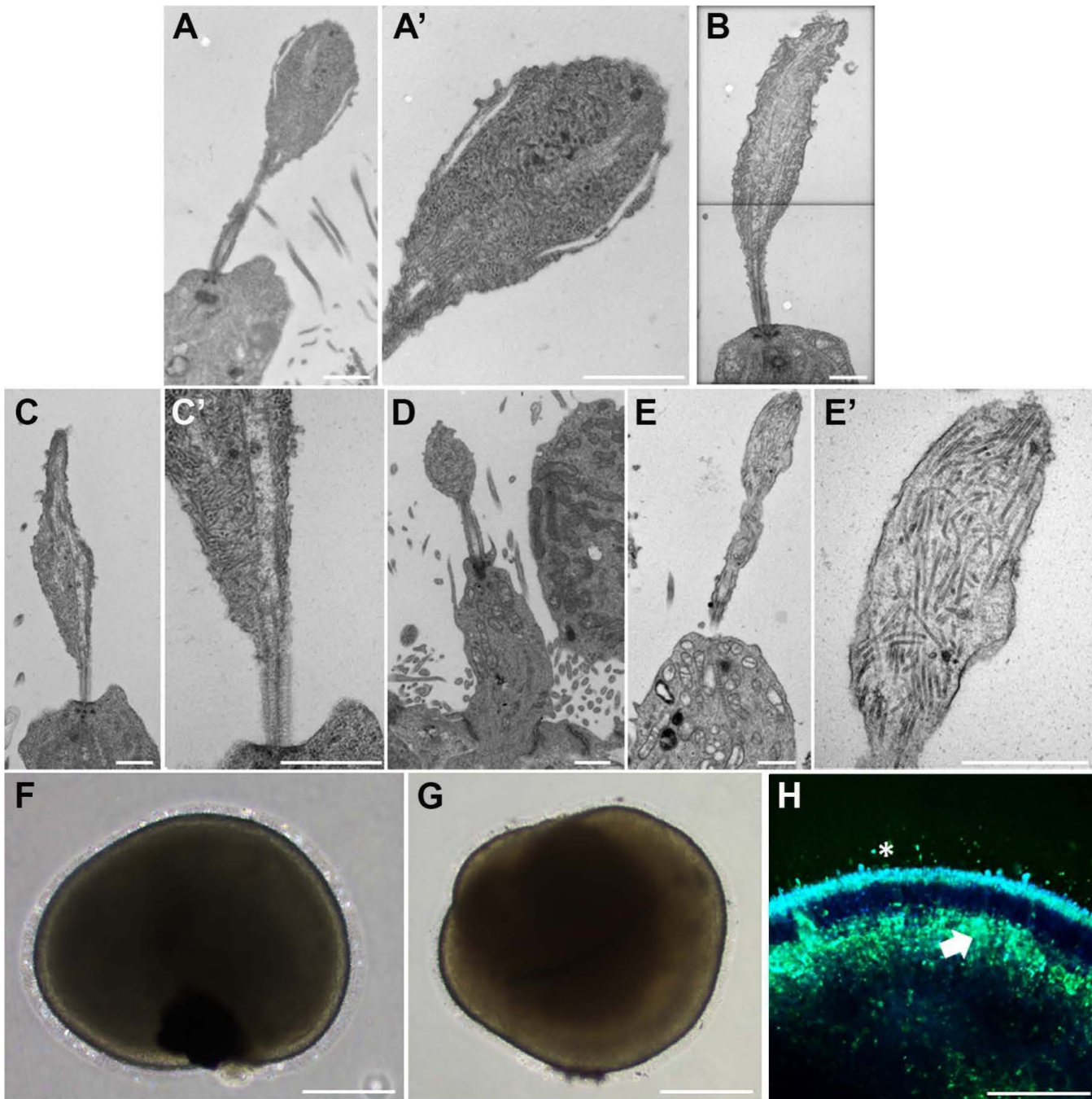


Figure S7. Examination of outer segment morphology and inner segment metabolic activity across multiple stage 3 organoids. (A-E') Electron micrographs of stage 3 organoid outer segments from five additional hPSC lines (scale bars = 800 nm). (F) LM image of the d250 stage 3 organoid shown in Figure 6M (scale bar = 150 μ m). (G, H) LM and optical metabolic imaging of a stage 3 organoid from an additional line showing metabolically active, NADP(H)-rich inner segments (blue) and retinol-containing regions (green) (scale bars: G = 200 μ m, H = 100 μ m).

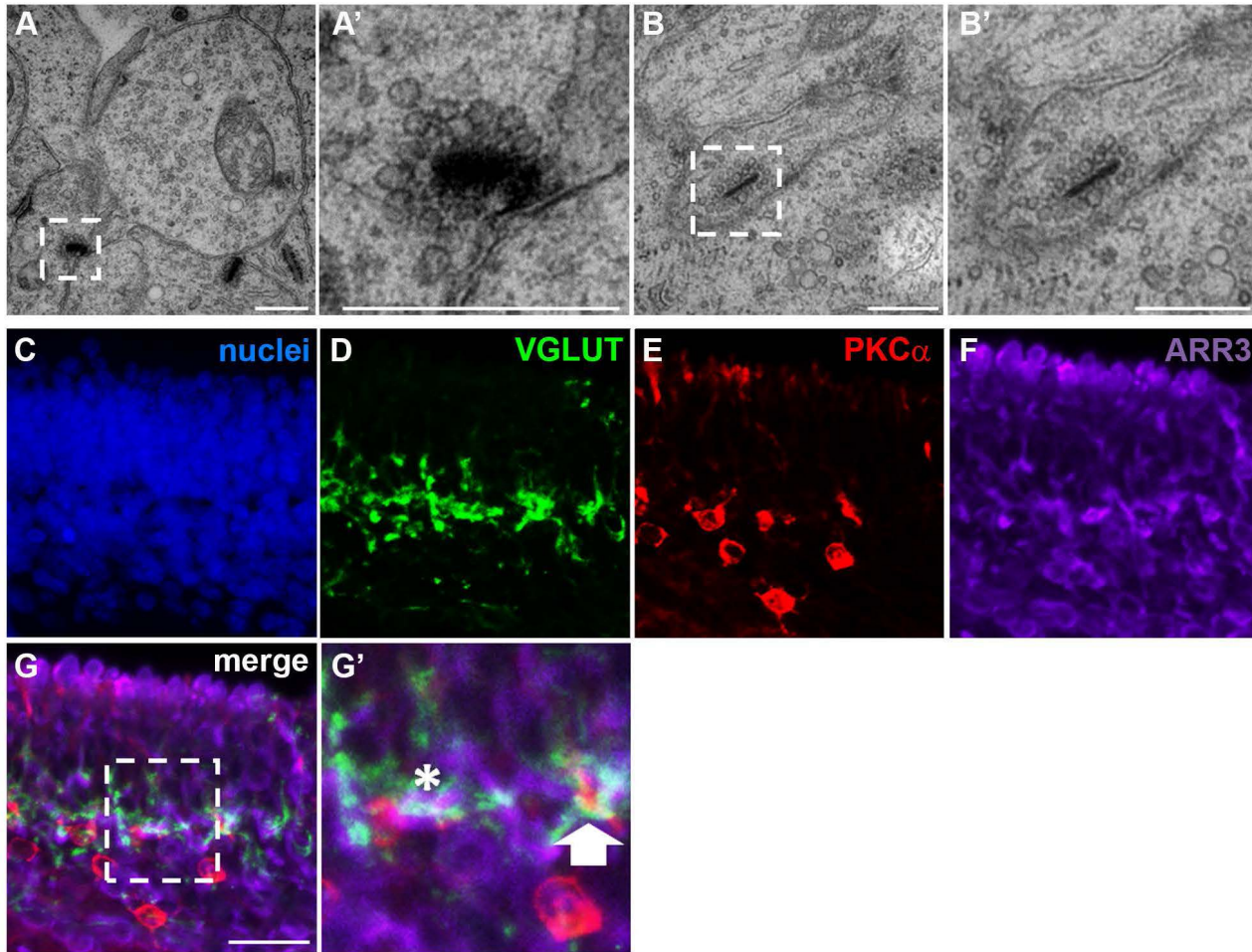


Figure S8. Further demonstration of ribbon synapses and BPCs in stage 3 organoids. (A-B')

Electron micrographs of stage 3 organoid ribbon synapses from two additional hPSC lines. Dashed boxes in panels A and B outline magnified regions shown in panels A' and B', respectively (scale bars = 500 nm). (C-G') ICC images from a d240 stage 3 organoid showing expression of the presynaptic marker VGLUT1 with ARR3 in cone pedicles (asterisk in G') and with the post-synaptic rod BPC marker PKC α (arrow in G'). Panel G' shows a magnification of the boxed region in panel G (scale bar = 25 μ m).

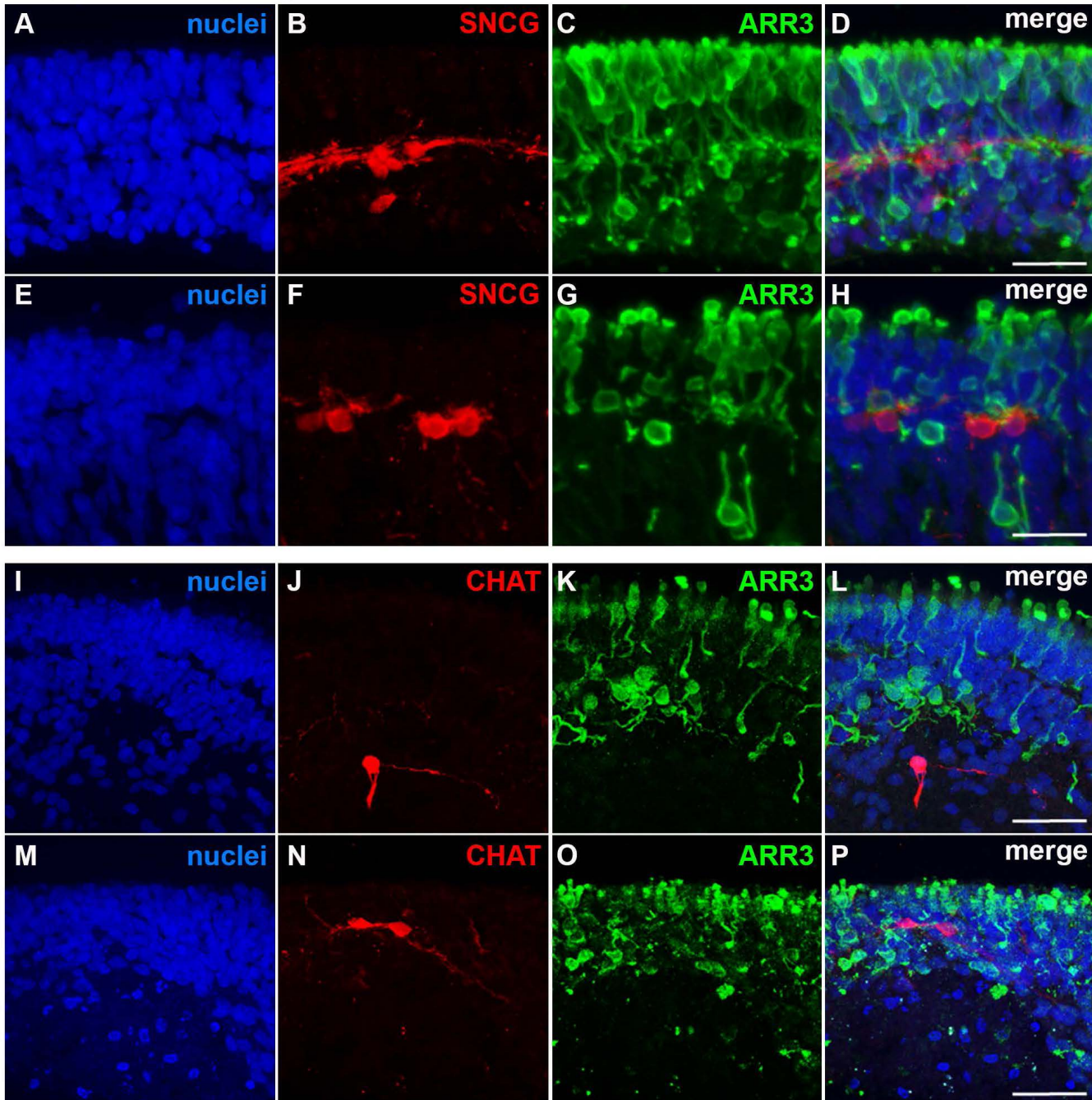
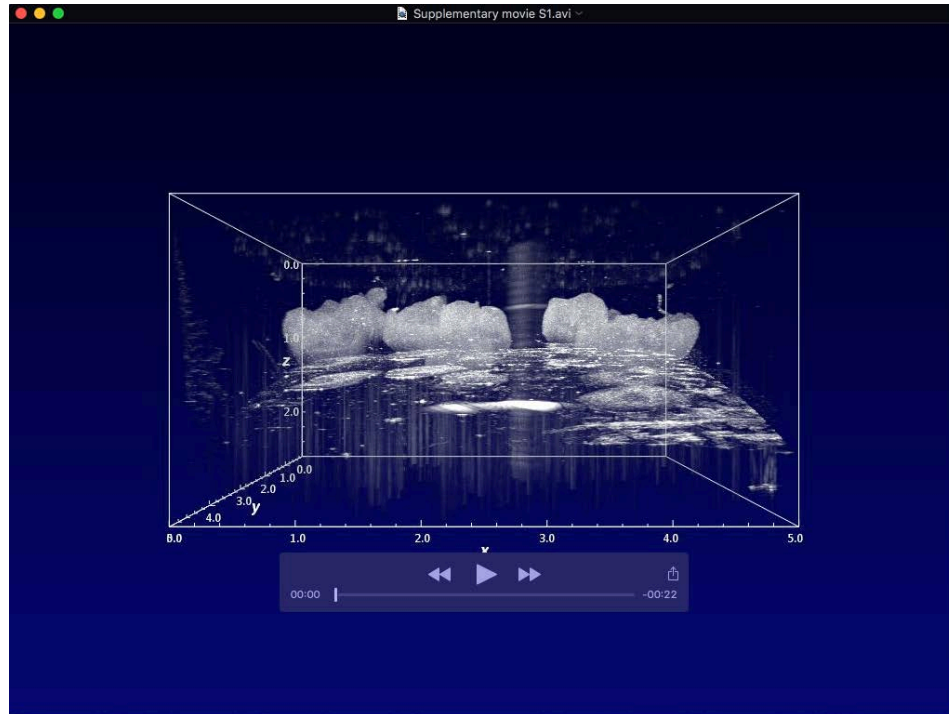
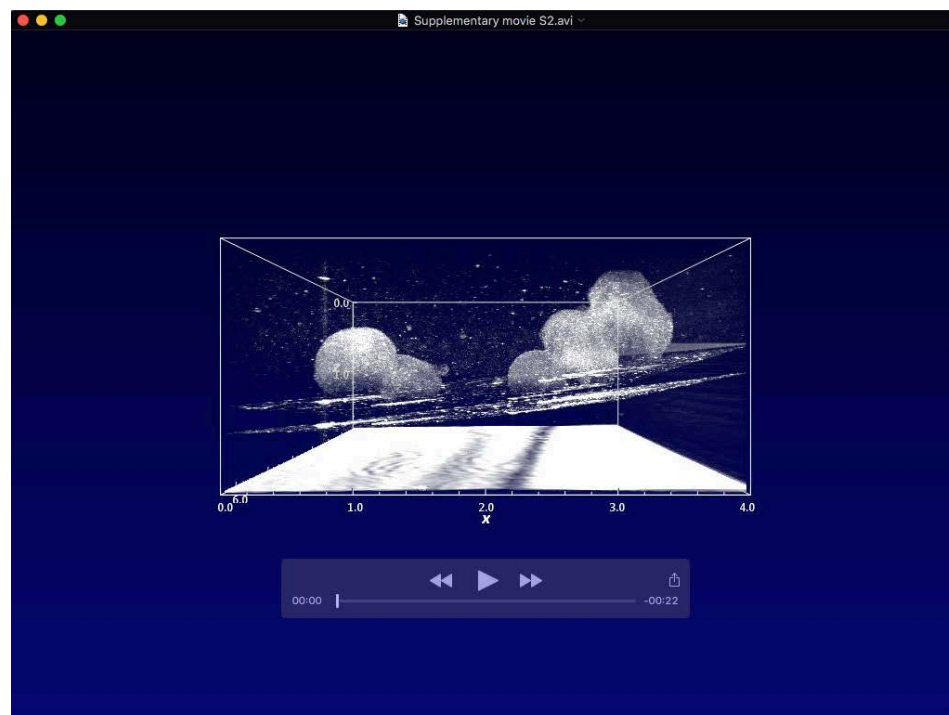


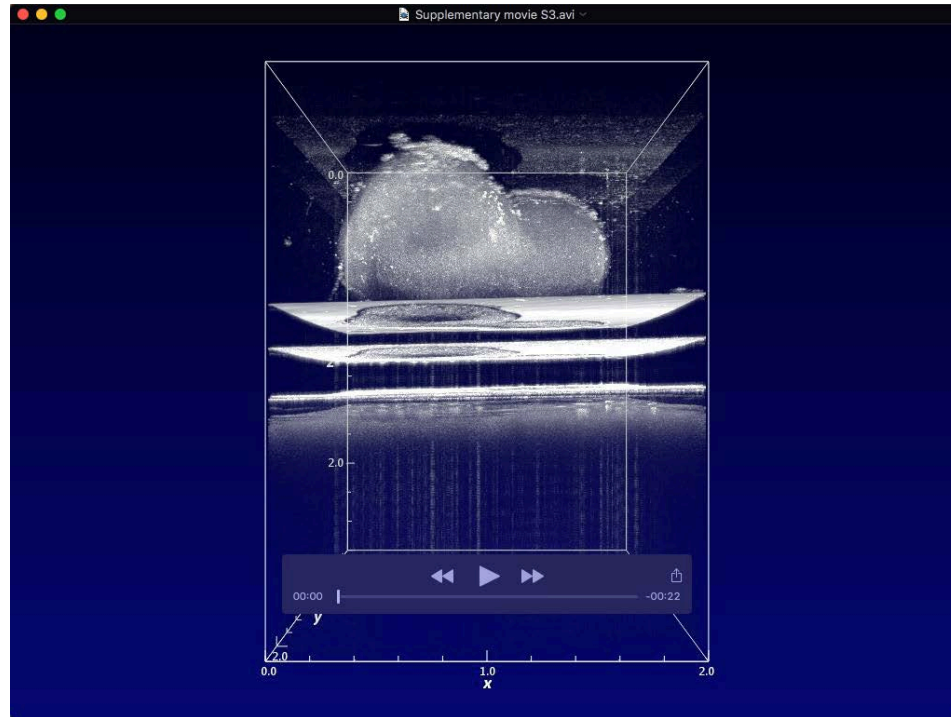
Figure S9. Further demonstration of RGC and SAC loss within inner organoid layers in hPSC lines. (A-H) RGC loss in stage 3 organoids from two additional hPSC lines (scale bar = 25 μm). (I-P) CHAT immunostaining showing the presence and morphology of rare SACs in stage 3 organoids from two additional hPSC lines (scale bar = 25 μm)



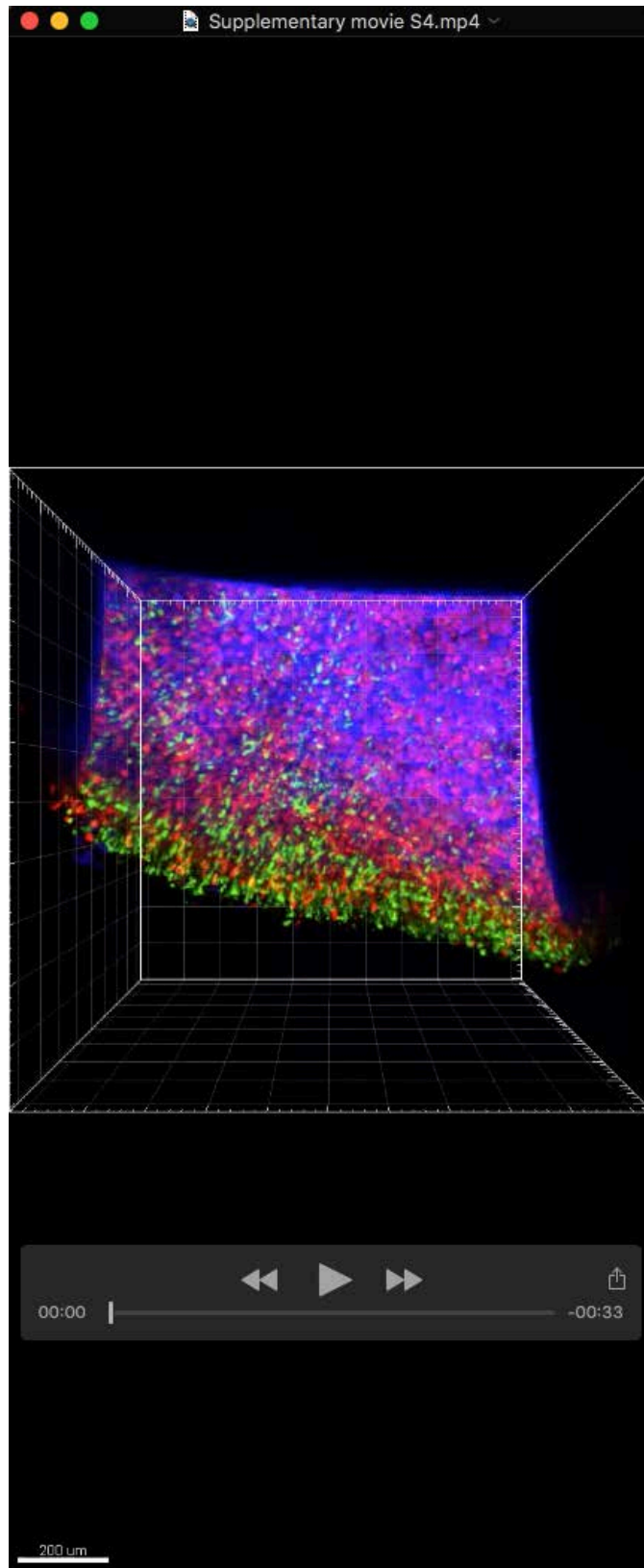
Movie 1. OCT analysis of stage 1 organoids. 3D OCT rendering of a group of stage 1 retinal organoids.



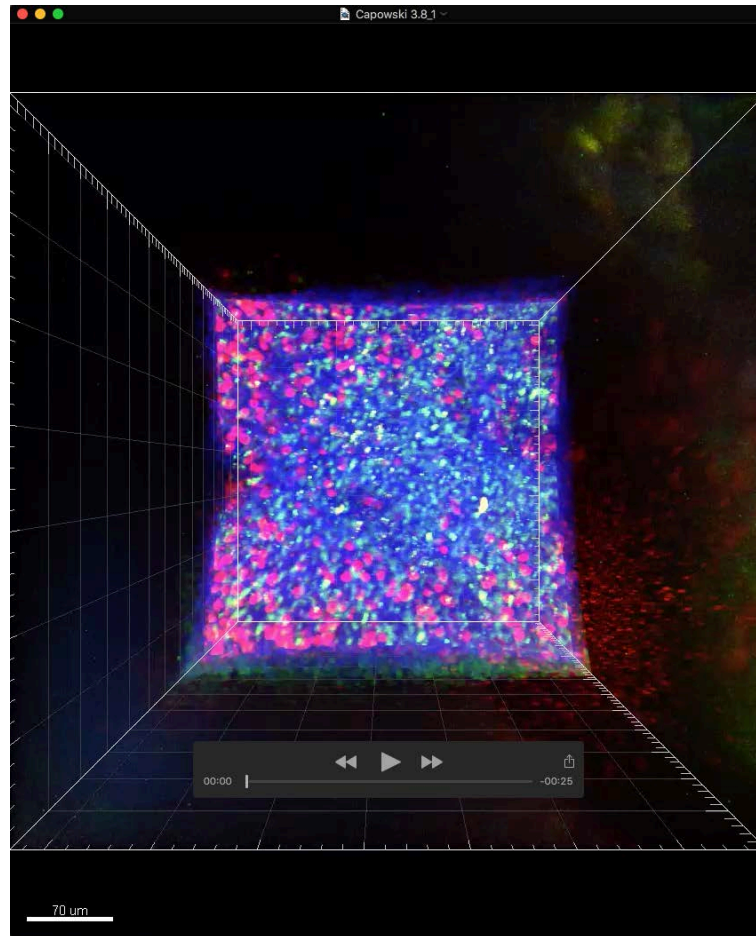
Movie 2. OCT analysis of stage 2 organoids. 3D OCT rendering of a group of stage 2 retinal organoids.



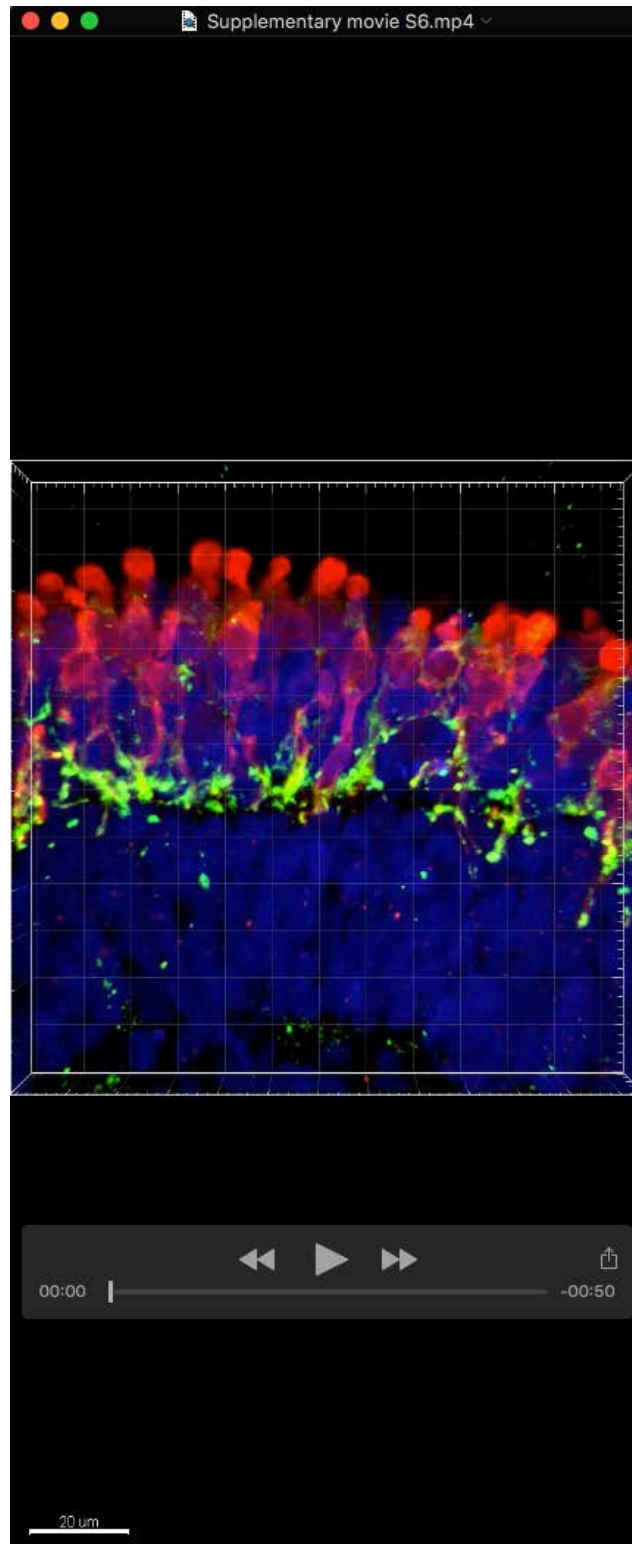
Movie 3. OCT analysis of a stage 3 organoid. 3D OCT rendering of a stage 3 retinal organoid.



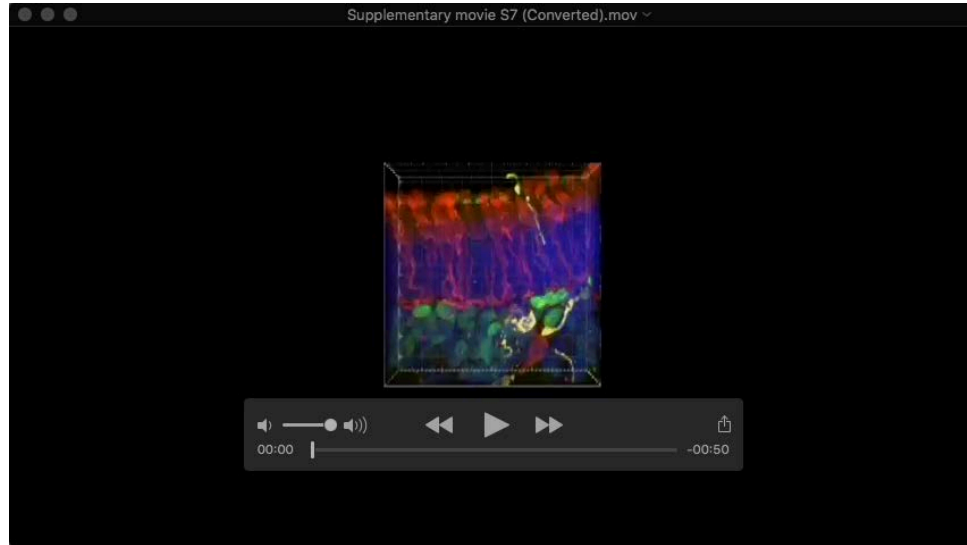
Movie 4. Immunocytochemical analysis reveals non-uniform distribution of opsins in a stage 3 organoid. 3D reconstruction of a multiphoton z stack showing the surface of a stage 3 (d241) retinal organoid, with expression of M/L OPSIN (red) and ROD OPSIN (green) relative to nuclei (blue).



Movie 5. Immunocytochemical analysis highlighting elongated photoreceptor outer segments in an advanced stage 3 organoid. 3D reconstruction of a multiphoton z stack showing the surface of an older stage 3 (d345) retinal organoid, with expression of M/L OPSIN (red) and ROD OPSIN (green) relative to nuclei (blue).



Movie 6. Immunocytochemical analysis of stage 3 organoids demonstrating the presence of an outer plexiform-like layer. 3D image of a confocal z stack of a thick section from a stage 3 retinal organoid showing expression of cone ARR3 (red) and the pre-synaptic marker VGLUT1 (green) relative to nuclei (blue).



Movie 7. Stage 3 organoids contain inner and outer nuclear layers with appropriate cell types. 3D reconstruction of a confocal z stack of a thick section from a stage 3 retinal organoid showing expression of cone ARR3 (red), ROD OPSIN (yellow) and VSX2 (bipolar cells; green) relative to nuclei (blue). Note the presence of pedicles associated with the ARR3+ cone axons vs. spherules associated with the ROD OPSIN+ rod axons present within the ONL of this organoid.

Table S1: Primary antibodies

Antibody	source	catalog number	dilution
ARL13b	Protein Tech	11711	1:500
Cone arrestin (ARR3)	Novus	NBP1-37003	1:200
Cone arrestin (ARR3)	LS Bio	LS-C368677	1:300
Calretinin (CaR)	Millipore	AB5054BD	1:500
CHAT	Millipore	AB144P	1:100
CRALBP	Abcam	AB15051	1:250
CRX	Abnova	H0001406-M02	1:1000
C-terminal binding protein 2 (CTBP2)	BD Biosciences	BD 612044	1:300
G0 α	Millipore	MAB3073	1:700
Ki67	Abcam	ab15580	1:100
NR2E3	Abcam	ab172542	1:300
NRL	R&D Systems	AF2945	1:300
Onecut1 (OC1)	R&D Systems	AF6277	1:300
Opsin ML	Millipore	AB5405	1:500
Opsin S	Millipore	AB5407	1:500
OTX2	R&D Systems	AF1979	1:200
Pericentrin (PCN)	Abcam	ab28144	1:500
PKC α	Sigma	P4334	1:50
Recoverin (RCVN)	Millipore	AB5585	1:2000
Rhodopsin (RHO)	Millipore	MABN15	1:100
RFP (tdTomato)	Rockland	600-401-378	1:300
tdTomato	Sicgen	AB8181-200	1:300
Synuclein γ (SNCG)	Abnova	H00006623-M01A	1:500
Vesicular glutamate transporter (VGLUT)	Millipore	AB5905	1:2000
VSX2	Exalpha	X1179P	1:200